
CORU: Comprehensive Post-OCR Parsing and Receipt Understanding Dataset

Abdelrahman Abdallah^{1*} Mahmoud Abdalla^{2*} Mahmoud SalahEldin Kasem^{3*}
Mohamed Mahmoud^{3*} Ibrahim Abdelhalim^{3*} Mohamed Elkasaby²
Yasser ElBendary² Adam Jatowt¹

¹University of Innsbruck ²DISCO Company
³Assiut University
abdelrahman.abdallah@uibk.ac.at, Adam.Jatowt@uibk.ac.at

Abstract

In the fields of Optical Character Recognition (OCR) and Natural Language Processing (NLP), integrating multilingual capabilities remains a critical challenge, especially when considering languages with complex scripts such as Arabic. This paper introduces the Comprehensive Post-OCR Parsing and Receipt Understanding Dataset (CORU), a novel dataset specifically designed to enhance OCR and information extraction from receipts in multilingual contexts involving Arabic and English. CORU consists of over 20,000 annotated receipts from diverse retail settings, including supermarkets and clothing stores, alongside 30,000 annotated images for OCR that were utilized to recognize each detected line, and 10,000 items annotated for detailed information extraction. These annotations capture essential details such as merchant names, item descriptions, total prices, receipt numbers, and dates. They are structured to support three primary computational tasks: object detection, OCR, and information extraction. We establish the baseline performance for a range of models on CORU to evaluate the effectiveness of traditional methods, like Tesseract OCR, and more advanced neural network-based approaches. These baselines are crucial for processing the complex and noisy document layouts typical of real-world receipts and for advancing the state of automated multilingual document processing. Our datasets are publicly accessible².

1 Introduction

Optical Character Recognition (OCR) [13, 7, 11] is the process of converting images of characters into digital texts. With the advent of deep learning and advancements in the field of computer vision, the performance of OCR has seen significant improvements. However, there is still room for enhancement, particularly in tasks that intersect with Natural Language Processing (NLP) and Information Extraction (IE) [13]. One of the most challenging in this domain is post-OCR parsing. This task involves predicting predefined semantic labels from the OCR output, a process that is far from straightforward. Existing datasets often fall short of providing a comprehensive environment for this research problem. For instance, OCR datasets typically lack parsing class labels. On the

*Equal contribution.

²<https://github.com/Update-For-Integrated-Business-AI/CORU>

other hand, the parsing datasets usually contain error-free texts, which do not accurately represent the error-prone outputs typical of OCR processes. In recent years, researchers from both OCR and NLP communities have been working to address this issue by compiling datasets with defined labels. Notable contributions in this area include the Scanned Receipts OCR and Information Extraction (SROIE) dataset [6] introduced by the ICDAR 2019 Post-OCR Challenge and the subsequent CORD dataset [15]. The above datasets provide a comprehensive collection of receipt images, accompanied by two distinct types of annotations aimed at addressing OCR and parsing problems. The first type of annotation provides box-level text annotations for OCR, while the second type is designed for parsing tasks.

In this paper, we introduce a novel dataset named CORU, standing for Comprehensive Post-OCR Parsing and Receipt Understanding. In the CORU dataset, we have collected a diverse array of receipt images from various retail environments. Figure 1 presents examples of these annotated receipt images, highlighting the variety of formats and the complexity of text layouts. To our knowledge, this is the first publicly available dataset explicitly designed to facilitate advanced post-OCR parsing and semantic understanding of receipts, integrating both English and Arabic texts. The detailed contributions of CORU are listed below:

- **Key Information Detection:** The first component of our dataset involves 20,000 human-annotated receipts. These annotations target the extraction of key information such as merchant names, dates, receipt numbers, items, and total prices.
- **Large-Scale OCR Dataset:** CORU includes a comprehensive set of 30,000 images for OCR tasks. This large-scale component is crucial for training and refining OCR systems to handle the specific challenges presented by receipts, such as diverse layouts and degraded text quality.
- **Detailed Item Analysis:** The dataset also provides detailed annotations for 10,000 items, focusing on extracting and classifying item-specific information. It involves classifying and extracting item-specific data, which is crucial for applications requiring item analysis and classification.
- **Baseline Performance Metrics:** We establish baseline performances using traditional and advanced neural network approaches for each of the three primary tasks—object detection, OCR, and information extraction.
- **OCR Model:** We introduce an OCR model designed to address the unique challenges of extracting text from receipts. This model leverages a combination of convolutional neural networks and bidirectional LSTMs, optimized to handle the diverse and noisy backgrounds often found in receipt images.



Figure 1: Examples of annotated receipt images from the CORU dataset. The images illustrate the variety of receipt formats and the complexity of text layouts.

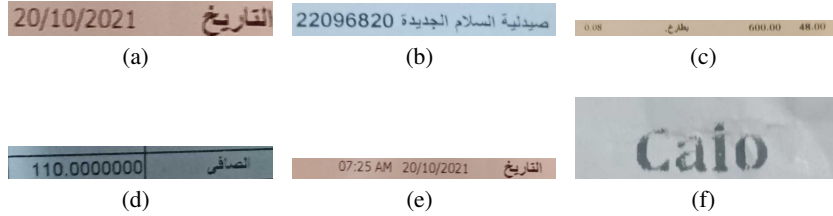


Figure 2: OCR images from receipt. Each subfigure shows a different example of the OCR task, including date, merchant, and items.

2 Related Work

While several datasets cater to various OCR tasks [13, 1], there is a notable shortage of receipt datasets, particularly for Arabic receipts. To highlight the unique features and comprehensive nature of our dataset, Table 1 compares it against existing datasets like SROIE, MC-OCR, UIT, and CORD. One of the earliest and most popular datasets in the scanned receipt domain is the ICDAR 2019 Challenge on Scanned Receipts OCR and Key Information Extraction (SROIE) dataset [6]. This dataset marked a significant advancement in the automated analysis of scanned receipts by introducing a standardized collection of 1,000 annotated receipt images. It focuses on three tasks: text localization, OCR, and key information extraction. These tasks are essential for document analysis systems with substantial commercial potential. The challenge emphasized the unique difficulties inherent in receipt OCR, such as poor scan quality and complex layouts. The CORD (Consolidated Receipt Dataset) dataset [15] addresses the challenge of integrating OCR with NLP tasks like semantic parsing by providing a comprehensive resource for post-OCR parsing. It includes thousands of Indonesian receipt images with box-level text annotations for OCR and multi-level semantic labels for parsing. Unlike traditional datasets, CORD bridges the gap between OCR and parsing, enabling the development of robust models that can handle OCR errors. It also introduces line annotations for converting two-dimensional OCR text into a well-ordered sequence, thereby enhancing parsing performance. The MC-OCR (Mobile Captured Receipt Recognition Challenge) dataset [20], featured at RIVF 2021 conference, includes 2,436 images of Vietnamese receipts captured via mobile devices. This dataset supports two tasks: predicting receipt quality and recognizing key information fields. UIT-MLReceipts dataset [12] addresses the need for a more extensive and carefully labeled dataset for extracting receipt information, overcoming the limitations of existing datasets like SROIE and CORD. With a focus on enriching the available data, UIT-MLReceipts has been compiled by sourcing receipts from various establishments such as restaurants, cafes, bookstores, and supermarkets, ensuring diversity in structure, color, font, and format. Additionally, images from social media groups were incorporated to further enhance dataset variability.

Table 1: Comparative overview of the CORU dataset against existing datasets such as SROIE, MC-OCR, UIT, and CORD, highlighting differences in the number of images, categories, and supported tasks. OB refers to Object detection and IE refers to Information Extraction.

Dataset Name	# Images	# categories	OB	OCR	IE	Item IE	Language
SROIE	1,000	4	✓	✓	✓	X	English
MC-OCR	2,436	4	X	✓	✓	X	English & Vietnamese
UIT	2,147	4	✓	✓	✓	X	English & Vietnamese
CORD	1,000	8	✓	✓	✓	X	English
CORU (ours)	20,000	5	✓	✓	✓	✓	English & Arabic

3 Dataset and Annotations

In this section, we detail the creation of CORU. Our methodology integrates rigorous data collection, annotation, and quality control processes, ensuring that CORU is both diverse and reflective of real-world scenarios. Below we outline the systematic steps in the development of the dataset.

Data Collection The initial phase involved gathering a large and diverse array of receipts through the DISCO application³, a platform that facilitates the uploading of receipt images by registered users.

³<https://discoapp.ai/>

We collected over 100k receipts from various commercial settings such as restaurants, supermarkets, and retail stores, ensuring a broad representation of industries, products, and transaction types to mimic the complexity found in everyday transaction documents.

Annotation Guidelines and Team Setup To ensure consistent and accurate annotations, we developed detailed annotation guidelines. These guidelines defined key elements for annotation, including merchant names, items, total prices, and dates. We assembled a team of expert annotators trained in these guidelines to maintain uniformity throughout the annotation process.

Receipt Selection and Quality Control Our team carefully reviewed each receipt against specific quality criteria such as text clarity, completeness of the image, and relevance (ensuring documents were receipts and not other types of bills).

Object Detection Annotation Using the MakeSense tool⁴, annotators constructed bounding boxes around each identified object on the receipts, subsequently saving these annotations in both YOLO and COCO formats. A secondary review team then examined the annotations to rectify any inaccuracies, ensuring the integrity of the data.

OCR Annotation As part of the OCR task, the dataset includes images annotated specifically for recognizing textual information such as dates, merchant names, and item details. Figure 2 showcases examples of OCR images, illustrating the challenges and complexity of text recognition. Each identified object or line was passed to a specialized OCR annotation team, which annotated each segment character by character. Due to the challenges posed by bi-directional text in Arabic and left-to-right English, we developed a custom system to annotate each word from left to right, recording the annotations in a structured list that maintains the positional integrity of the words as they appear on the receipt.

Item-Specific Annotation Detailed annotations were applied to each receipt element such as item names, classifications, quantities, unit sizes, prices, packaging, and brands. A team of five annotators was tasked with this annotation job, using the established guidelines to ensure a consistent and accurate approach across all receipts.

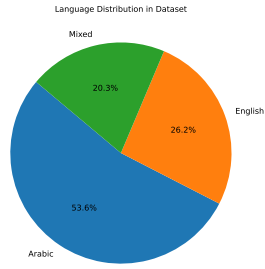
4 Dataset Analysis

In this section, we delve into the statistical and qualitative analysis of the CORU dataset. The cumulative distribution of classes (Figure 4(b)) reveals a progressive increase in class representation, with a steep rise observed at higher class IDs. This indicates a predominance of item classes within the dataset. The distribution across various item classes is depicted in Figure 3(b). It shows significant variation in the frequency of item types, from 'Soft drinks' and 'Rice, pasta, and noodles', which are notably prevalent, to less frequent categories like 'Hair & body care' and 'Tea & Coffee.' This diversity is important for developing models that are not only accurate but also versatile in handling a wide range of commercial products. Figure 4(a) presents the frequency of different object classes such as 'Date,' 'Item,' 'Merchant,' 'Receipt Number,' and 'Total.' Notably, 'Item' class entries are most frequent, underscoring the dataset's design towards detailed, item-level transaction analysis. This focus is instrumental for applications requiring fine-grained analysis like itemized billing and inventory management. The language composition of the dataset is useful for its application in multilingual OCR tasks. As shown in Figure 3(a), Arabic is the predominant language, comprising 53.6% of the dataset, followed by English at 26.2%, and mixed-language content at 20.3%. This multilingual aspect demonstrates the dataset's applicability in diverse linguistic settings, challenging the models to accurately process and understand content in multiple languages and their combinations.

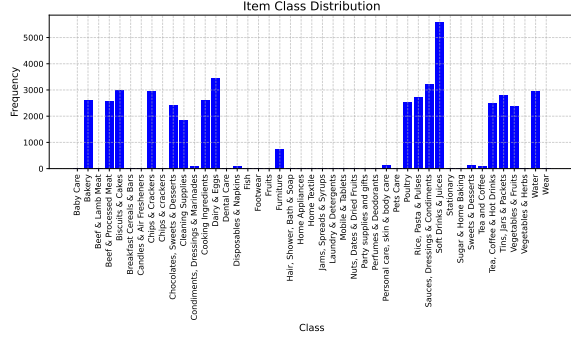
5 Models

In this section, we present a detailed exploration of various deep learning models that have been evaluated using the CORU dataset. Each model has been selected based on its potential to address specific challenges in OCR, object detection, and information extraction from multilingual receipts. We include a mix of traditional approaches, such as Tesseract OCR [16], and advanced neural network architectures, which leverage recent innovations in deep learning to improve accuracy and efficiency. Our evaluation spans a variety of model types, from convolutional neural networks (CNNs) [14] and Transformers to cutting-edge language models, providing insights into their performance across different computational tasks and conditions outlined in the CORU dataset.

⁴<https://www.makesense.ai/>

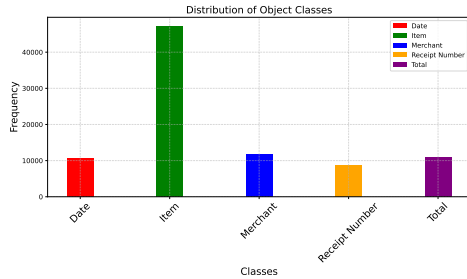


(a) Language Distribution in CORU

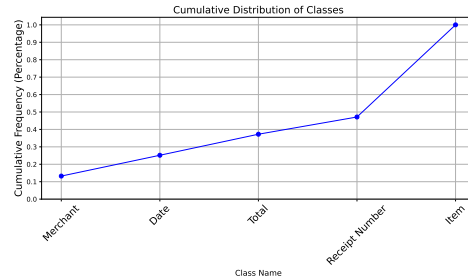


(b) Item Class Distribution in CORU

Figure 3: Distribution of language and item classes in the CORU dataset. Panel (a) displays the language distribution across the dataset, showing a mix of Arabic, English, and bilingual receipts. Panel (b) illustrates the distribution of item classes, reflecting the diversity in products in the receipts.



(a) Distribution of Object Classes in CORU



(b) Cumulative Distribution of Classes in CORU

Figure 4: Analysis of object classes and their cumulative distribution in the CORU dataset. Figure (a) shows the frequency of different object classes such as 'Date', 'Item', 'Merchant', etc. Figure (b) presents the cumulative distribution of these classes.

5.1 Object Detection Models

Weakly supervised object localization refers to the task of identifying object locations in images using only image-level labels rather than precise pixel-level annotations [23, 4]. The model learns to detect objects by classifying image patches and determining their relevance to the overall image label, making it a form of multiple instance learning.

CAM [27] revisits the global average pooling layer and shows how it enables the convolutional neural network (CNN) to have remarkable localization ability despite being trained on image-level labels. The key formula can be represented as follows: $f_k = \frac{1}{Z} \sum_i \sum_j f_k(i, j)$ where f_k is the k -th feature map of size $W \times H$ (width and height), and $Z = W \times H$ is the normalization constant.

HAS [17] introduces the 'Hide-and-Seek' framework that improves object localization by hiding patches in a training image randomly, and forcing the network to seek other relevant parts when the most discriminative part is hidden.

Adversarial Complementary Learning (ACoL) [25] automatically localizes integral objects of semantic interest with weak supervision. The key idea is to hide the most discriminative part from the model to capture the object's integral extent. The concept behind this solution involves two classifiers working in tandem, with one classifier's output guiding the erasure operation on the feature maps fed into the other classifier.

Self-produced Guidance (SPG) [26] masks separately the foreground, the object of interest, from the background to provide the classification networks with spatial correlation information of pixels.

The concept involves generating guidance masks based on attention maps and using these masks as auxiliary pixel-level supervision to facilitate the training of classification networks.

Attention-based Dropout Layer (ADL) [5] utilizes the self-attention mechanism to process the feature maps of the model. The key concept involves applying a dropout layer based on the attention map of the input, forcing the model to pay attention to less discriminative parts of the object.

CutMix [22] augmentation strategy, where patches are cut and pasted among training images and the ground truth labels are also mixed proportionally to the area of the patches. The key equation can be represented as follows: $\text{CutMix Image} = M \odot \text{Image}_1 + (1 - M) \odot \text{Image}_2$ where M is a binary mask indicating the cut and paste regions, \odot denotes element-wise multiplication, and Image_1 and Image_2 are the original and target images, respectively.

DETR [3] the vision transformer model with Improved Denoising Anchor Boxes (DINO) [24] employs a Transformer-based architecture that dynamically updates 4D anchor boxes through its decoder, using deformable attention to leverage multi-scale features effectively. DINO accelerates convergence through a contrastive denoising training method, optimizing detection by managing hard negatives with hyper-parameters λ_1 and λ_2 . The mathematical expression for the anchor tracking discrepancy (ATD) is given by: $\text{ATD}(k) = \frac{1}{k} \sum_{\text{topK}} \{\|b_0 - a_0\|_1, \|b_1 - a_1\|_1, \dots, \|b_{N-1} - a_{N-1}\|_1\}$ Additionally, the look-forward-twice strategy updates bounding box predictions iteratively as follows: $\Delta b_i = \text{Layer}_i(b_{i-1})$, $b'_i = \text{Update}(b_{i-1}, \Delta b_i)$ and $b_i = \text{Detach}(b'_i)$, $b_i^{\text{pred}} = \text{Update}(b'_{i-1}, \Delta b_i)$ This method ensures precise object localization, particularly useful in complex applications such as receipt item detection.

One-Stage Object Detection The advancements in one-stage object detection have been notably driven by the introduction of YOLOv7 [21] and YOLOv8 [10], marking significant milestones in real-time object detection technologies. YOLOv7 improves upon its predecessors by implementing the Focus (Fu) module, which utilizes spatial attention mechanisms to dynamically enhance focus on relevant regions within feature maps, leading to more precise object localization. This is expressed in the equation $F_k(i, j) = \sigma(\sum_{m=1}^C w_m^k f_m(i, j))$, where each component plays a specific role in enhancing detection precision. The model also incorporates a Path Aggregation Network (PAN) and Efficient Bottleneck ($E - B$) to further optimize performance across various object sizes and improve computational efficiency. On the other hand, YOLOv8 employs CSPDarknet53 as its backbone, which is crucial for multi-scale feature extraction and includes the newly introduced C2f module, enhancing the model’s non-linear representation capabilities. This backbone processes input images at multiple resolutions to detect objects at different scales with high accuracy, and its design incorporates multiple bottleneck blocks that split and concatenate feature maps, optimizing the final convolution layer outputs for accurate detection across diverse object instances. Together, YOLOv7 and YOLOv8 represent a leap forward in the field, combining innovative architectural elements to set new benchmarks for speed and accuracy in object detection.

5.2 OCR

The OCR model combines convolutional neural networks (CNNs) and Long Short-Term Memory (LSTM) units to enhance text extraction and recognition capabilities for optical character recognition (OCR) tasks. We build an OCR Model which contains a convolutional layer designed to perform initial feature extraction. This layer applies multiple filters to the input image, capturing essential textual features such as edges and textural details. The convolution operation can be mathematically represented as: $f(x, y) = \sum_{i=-a}^a \sum_{j=-b}^b k(i, j) \cdot g(x - i, y - j)$ where $f(x, y)$ denotes the output feature map, $g(x, y)$ the input image, and $k(i, j)$ the convolutional filter. This operation is critical for detecting patterns that form the basis for character recognition. Following the convolutional layer, the extracted features are processed by LSTM units. These units are crucial for managing the sequence data, effectively capturing both short-term and long-term textual dependencies. Using bidirectional LSTMs ensures that the context from all directions is considered, enhancing the model’s ability to decode text sequences accurately.

5.3 LLM models

Llama [18]⁵ is a part of the Llama 2 family of Large Language Models (LLMs) developed by Meta. These models are pre-trained and fine-tuned generative text models, specifically optimized for dialogue use cases. They have demonstrated superior performance on numerous benchmarks. The models employ supervised fine-tuning and reinforcement learning with human feedback to align with human preferences for helpfulness and safety. **Mistral** [8]⁶, a model released by Mistral AI, is renowned for its power and efficiency. It surpasses the Llama 2 13B on all benchmarks. The model leverages instruction fine-tuning, where the prompt should be surrounded by [INST] and [/INST] tokens. **Mixtral** [9]⁷, another innovation from Mistral AI, is a trained generative Sparse Mixture of Experts that outperforms the Llama 2 70B model on most benchmarks. The model leverages up to 45B parameters but only uses about 12B during inference, leading to better inference throughput at the cost of more vRAM. **Falcon** [2]⁸ is a class of causal decoder-only models. The largest Falcon checkpoints have been trained on more than 1T tokens of text, with a particular emphasis on the RefinedWeb corpus. Falcon architecture is modern and optimized for inference, with multi-query attention and support for efficient attention variants like FlashAttention. **Zephyr** [19]⁹ is a state-of-the-art model developed by the Hugging Face. It is designed for a wide range of natural language processing tasks, including text generation, translation, and summarization. The model leverages the Transformer architecture, which allows it to capture long-range dependencies in the input text. The Zephyr model is pre-trained on a large corpus of text and can be fine-tuned for specific tasks.

6 Experimental Results

In this section, we discuss our experimental results using the models described above.

6.1 Object Detection Results

The object detection models we evaluated include Class Activation Mapping (CAM), Hide-and-Seek (HAS), Attention-based Dropout Layer (ADL), Adversarial Complementary Learning (ACOL), Self-produced Guidance (SPG), CutMix, and DETR with Improved Denoising Anchor Boxes (DINO), each employing different architectures like ResNet50, VGG16, InceptionV2, and Swin Transformer. Our evaluation focuses on both classification and localization metrics. Table 2 shows a detailed comparison of object detection performance across various models and backbone configurations. For instance, the DINO model equipped with the Swin 4-scale backbone shows a better average score of 32.2, with notable robustness across different quality thresholds—45.4 at 10%. In contrast, traditional models like CAM and HAS, while effective to a certain degree, have limitations with ResNet50 scoring an average of 6.17 and 7.14, respectively, with performance dropping significantly at higher quality thresholds. Our evaluation of the YOLO models provided significant insights into real-time object detection capabilities within the CORU dataset. In Table 6, YOLOv7 demonstrated the highest performance metrics in terms of precision (P), recall (R), and mean Average Precision (mAP) at IoU=0.50 (mAP50), pointing to robustness in detecting various objects on multilingual receipts with diverse layouts. Although YOLOv8 showed slightly lower performance compared to YOLOv7, it offered improvements in mAP across different IoU thresholds (mAP50-95), suggesting better generalization across diverse object sizes and shapes. YOLOv9 further improved upon these metrics, highlighting the continuous advancements in the YOLO architecture to enhance detection accuracy and efficiency in challenging OCR scenarios.

Table 4 shows the object classification accuracy for various detection methods across different backbone architectures. CAM reveals strong and consistent performance, with scores of 43.10 for ResNet50 and 43.74 for VGG16. Conversely, the Hide-and-Seek (HAS) method displays significant variability, excelling with a score of 34.15 on ResNet50 but performing poorly with VGG16, where it achieves accuracy of only 16.36. This indicates the dependency of HAS’s effectiveness on the backbone’s feature extraction capability. Advanced methods such as the Attention-based Dropout Layer (ADL) and Adversarial Complementary Learning (ACOL) both perform well, particularly with

⁵<https://huggingface.co/meta-llama/Llama-2-7b-chat-hf>

⁶<https://huggingface.co/mistralai/Mistral-7B-Instruct-v0.2>

⁷<https://huggingface.co/mistralai/Mixtral-8x7B-Instruct-v0.1>

⁸https://huggingface.co/docs/transformers/main/model_doc/falcon

⁹https://huggingface.co/docs/transformers/main/model_doc/zephyr

Table 2: Comparative Analysis of Object Detection Models Across Different Backbone Architectures. This table provides detailed metrics for various object detection models using backbone networks such as ResNet50, VGG16, InceptionV2, and Swin Transformer. Each row represents a different model, evaluating performance at multiple quality thresholds to illustrate their effectiveness in localizing key objects within complex receipt images.

Method	Backbone	Avg	IoU								
			10	20	30	40	50	60	70	80	90
CAM	ResNet50	6.17	41.08	11.93	4.48	2.24	1.07	0.59	0.21	0.05	0.05
	VGG16	5.86	45.23	10.12	2.24	0.64	0.16	0.11	0.05	0.00	0.00
	InceptionV2	5.26	36.81	9.06	3.52	1.76	0.80	0.37	0.21	0.05	0.00
HAS	ResNet50	7.14	43.26	16.84	6.55	2.72	1.17	0.59	0.21	0.11	0.00
	VGG16	0.00	0.00	0.00	0.00	0.00	0.00	0.00	0.00	0.00	0.00
	InceptionV2	4.65	34.79	8.20	2.40	0.75	0.21	0.11	0.05	0.00	0.00
ADL	ResNet50	6.57	39.74	15.13	6.34	2.56	1.17	0.48	0.16	0.11	0.05
	VGG16	6.97	47.52	15.34	4.69	1.60	0.37	0.16	0.05	0.00	0.00
	InceptionV2	7.04	52.10	11.61	4.00	1.60	0.64	0.27	0.11	0.05	0.00
ACOL	ResNet50	3.94	27.49	7.19	2.72	1.01	0.48	0.32	0.21	0.00	0.00
	VGG16	0.00	0.00	0.00	0.00	0.00	0.00	0.00	0.00	0.00	0.00
	InceptionV2	7.04	52.10	11.61	4.00	1.60	0.64	0.27	0.11	0.05	0.00
SPG	ResNet50	6.53	42.14	13.00	5.06	2.66	1.33	0.64	0.27	0.11	0.05
	VGG16	-	-	-	-	-	-	-	-	-	-
	InceptionV2	4.74	35.11	7.73	2.66	1.07	0.48	0.27	0.05	0.00	0.00
Cutmix	ResNet50	6.32	41.61	13.37	5.01	1.97	0.69	0.37	0.16	0.05	0.00
	VGG16	5.54	38.47	11.45	3.25	1.28	0.59	0.27	0.11	0.00	0.00
	InceptionV2	4.64	31.91	8.42	3.57	1.55	0.59	0.27	0.05	0.00	0.00
DINO	Swin 4-scale	32.2	45.4	44.6	43.3	41.9	39.9	35.9	27.5	10.6	0.7
	ResNet50 4-scale	31.9	45.9	45.0	43.6	41.9	39.4	35.2	25.6	10.2	0.5
	ResNet50 5-scale	29.4	44.1	43.2	41.7	39.8	37.1	32.5	25.0	0.89	0.00

Table 3: Performance Metrics for Few-shot Information Extraction Across Multiple Categories

Models	parameters	#Shots	Brand		Weight		# Units		S.Units		T.Price		Price		Pack		Units		Overall	
			F1	Acc	F1	Acc	F1	Acc	F1	Acc	F1	Acc	F1	Acc	F1	Acc	F1	Acc	F1	Acc
LLaMA V1	7B	0	3.70	0.93	4.29	1.25	8.14	3.34	0.04	0.02	0.08	0.04	0.08	0.04	0.08	0.04	0.00	0.00	0.88	0.46
LLaMA V2	7B	0	29.16	16.46	28.32	15.87	74.94	60.52	0.04	0.02	0.75	0.38	1.50	0.75	0.33	0.17	2.39	0.24	20.70	10.80
Mistral	7B	0	14.46	6.97	11.70	5.35	54.00	36.89	0.00	0.00	0.79	0.40	0.67	0.34	0.17	0.08	7.19	2.82	12.14	5.61
Mixtral	8x7B	0	32.07	18.53	25.66	14.05	82.64	71.37	0.21	0.10	1.50	0.75	1.95	0.98	0.67	0.34	16.52	8.20	24.53	13.29
Falcon	7B	0	28.98	16.33	20.93	10.95	69.35	53.46	0.08	0.04	1.08	0.54	2.07	1.05	0.08	0.04	0.65	0.34	18.18	9.22
Zephyr	7B	0	29.88	16.96	18.60	9.48	48.80	32.05	0.25	0.13	0.88	0.44	0.96	0.48	0.88	0.44	0.00	0.00	13.24	6.25
			42.98	27.02	33.89	19.87	77.88	64.50	0.17	0.08	0.96	0.48	1.54	0.78	0.88	0.44	24.85	13.50	26.82	14.83
LLaMA V1	7B	1	47.27	30.68	57.56	40.41	42.02	26.22	76.32	62.36	84.92	74.87	84.92	74.87	6.51	2.44	0.08	0.04	55.89	38.74
LLaMA V2	7B	1	38.90	23.71	41.35	25.68	61.82	44.87	43.48	27.44	67.27	50.99	65.18	48.58	2.63	0.37	13.29	6.28	44.73	28.49
Mistral	13B	1	41.51	25.80	51.86	34.85	75.58	61.38	66.42	50.00	80.06	67.58	79.34	66.55	2.83	0.47	36.26	21.65	58.18	41.04
Mixtral	7B	1	39.32	24.04	55.80	38.65	75.44	61.19	68.70	52.68	87.53	79.04	81.22	69.25	5.62	1.96	36.29	21.67	60.60	43.56
Zephyr	8x7B	1	46.86	30.33	58.07	40.93	34.54	20.35	77.36	63.79	92.33	87.27	92.39	87.38	5.31	1.79	0.77	0.40	58.54	41.41
LLaMA V1	7B	2	42.75	26.82	71.73	56.39	79.40	66.63	82.29	70.84	87.50	78.99	87.42	78.87	41.58	25.86	0.0	0.0	66.68	50.30
LLaMA V2	7B	2	52.17	35.14	72.19	56.97	93.42	89.24	80.64	68.41	94.05	90.41	94.16	90.60	53.40	36.31	50.95	34.01	76.52	62.64
Mistral	13B	2	51.22	34.26	74.33	59.72	93.06	88.59	94.01	90.33	95.16	92.48	95.07	92.32	13.53	6.42	45.55	29.19	75.80	61.66
Mixtral	7B	2	49.33	32.52	73.29	58.38	91.48	85.76	89.79	82.83	94.58	91.40	94.74	91.69	41.66	25.92	47.71	31.08	76.38	62.45
Falcon	8x7B	2	43.35	27.33	63.07	46.22	78.68	65.63	69.60	53.77	84.00	73.44	83.86	73.23	10.12	4.45	27.41	15.24	61.86	44.91
Zephyr	7B	2	47.95	31.29	65.01	48.38	81.85	70.19	89.78	82.81	85.98	76.54	84.93	74.89	13.78	6.56	0.12	0.06	65.19	48.59
			52.43	35.39	71.31	55.86	92.57	87.71	90.87	84.69	94.95	92.09	94.90	91.98	57.36	40.21	63.35	46.54	79.52	66.81
LLaMA V1	7B	3	44.45	28.25	64.32	47.61	83.55	72.75	90.72	84.44	89.96	83.12	89.76	82.78	37.07	22.28	0	0	68.47	52.40
LLaMA V2	7B	3	52.43	35.39	71.31	55.86	92.57	87.71	90.87	84.69	94.95	92.09	94.90	93.98	57.36	40.21	63.35	46.54	79.52	66.81
Mistral	13B	3	49.49	32.67	66.53	50.12	93.71	89.78	96.19	94.45	95.17	92.51	95.12	92.40	41.07	25.44	53.69	36.59	77.69	64.25
Mixtral	7B	3	51.88	34.87	76.11	62.08	92.05	86.77	94.59	91.42	95.08	92.34	94.88	91.96	49.90	33.05	66.85	50.50	80.26	67.87
Falcon	8x7B	3	51.65	34.66	69.71	53.89	87.24	78.57	80.13	67.68	93.28	88.99	93.15	88.76	20.40	10.61	29.61	16.77	70.60	54.99
Zephyr	7B	3	62.30	45.39	63.68	46.90	91.73	86.20	95.79	93.68	93.34	89.09	93.31	89.05	14.88	7.21	0.0	0.0	72.16	56.94
			56.36	39.21	72.24	57.04	84.20	73.75	87.64	79.22	93.93	90.18	93.86	90.05	57.22	40.06	51.67	34.68	76.80	63.02

InceptionV2, each with 42.09, suggesting that methods which diversify the model’s attention across the image can significantly improve classification outcomes in complex datasets like CORU.

6.2 OCR Results

The OCR task of the CORU dataset is important for information extraction. Table 5 summarizes the Character Error Rate (CER) and Word Error Rate (WER) metrics of various OCR models. As a baseline, Tesseract OCR shows a Character Error Rate (CER) of 15.56% and a Word Error Rate (WER) of 30.78%. While Tesseract is widely used due to its open-source nature and extensive language support, the Attention-Gated CNN-BiGRU model improves upon the baseline, reducing the CER to 14.85% and the WER to 27.22%. This model combines gated convolutional neural networks with bidirectional GRU layers, enhanced by attention mechanisms, which likely contributes to its improved handling of spatial dependencies and contextual information within the text. Our OCR Model, designed specifically for the challenges presented by the CORU dataset, further reduces the CER to 7.83%. However, its WER is comparable to that of the Attention-Gated CNN-BGRU at 27.24%, suggesting that while it is more adept at recognizing individual characters, it struggles

similarly at the word level. Azura OCR achieves the best performance among the tested models, with the lowest CER of 6.39% and WER of 25.97%.

Table 4: Performance Comparison of Object Classification Methods Across Different Backbone Architectures.

Method	ResNet50	VGG16	InceptionV2
CAM	43.10	43.74	38.46
HAS	34.15	16.36	40.65
ADL	41.72	41.56	42.09
ACOL	43.74	16.36	42.09
SPG	42.19	-	40.92
Cutmix	41.45	41.93	40.60

Table 5: OCR Performance Comparison

Model	CER (%)	WER (%)
Tesseract OCR	15.56	30.78
Attention-Gated	14.85	27.22
Our OCR Model	7.83	27.24
Azura OCR	6.39	25.97

Table 6: Performance Evaluation of YOLO Models

Model	P	R	mAP50	mAP50-95
YoloV7	76.00	85.60	79.20	43.70
YoloV8	74.60	81.00	76.10	45.30
YoloV9	75.70	83.40	77.90	46.70

6.3 Information Extraction Results

The exploration of information extraction capabilities of language models across zero-shot, one-shot, and few-shot scenarios reveals significant insights into their adaptability and effectiveness. In zero-shot learning, models generally struggle with precision and recall in complex categories like 'Brand' and 'Weight', with Zephyr and Falcon showing relatively better generalization capabilities. The one-shot scenario indicates improvements across the board, with LLaMA V1 demonstrating considerable robustness. Few-shot learning results, detailed in Table 3, demonstrate enhancements in model performance as they were exposed to more examples, affirming the value of incremental learning in complex extraction tasks. These observations underscore the capabilities of current language models to adapt to the demands of extracting structured information from unstructured datasets like receipts.

7 Conclusion

In this work, we presented CORU, a comprehensive dataset designed for enhancing OCR and post-OCR processing in multilingual contexts, particularly involving Arabic and English texts. Our dataset, comprising over 20,000 annotated receipts, supports a range of computational tasks including object detection, OCR, and detailed information extraction. We introduced several models and evaluated their performance across these tasks, demonstrating also the capabilities of our novel OCR model and various object detection frameworks. The results underscore the potential of CORU to facilitate advanced research and practical applications in document understanding and automation.

References

- [1] Abdelrahman Abdallah, Daniel Eberharter, Zoe Pfister, and Adam Jatowt. Transformers and language models in form understanding: A comprehensive review of scanned document analysis. *arXiv preprint arXiv:2403.04080*, 2024.
- [2] Ebtesam Almazrouei, Hamza Alobeidli, Abdulaziz Alshamsi, Alessandro Cappelli, Ruxandra Cojocaru, Mérouane Debbah, Étienne Goffinet, Daniel Hesslow, Julien Launay, Quentin Malartic, et al. The falcon series of open language models. *arXiv preprint arXiv:2311.16867*, 2023.
- [3] Nicolas Carion, Francisco Massa, Gabriel Synnaeve, Nicolas Usunier, Alexander Kirillov, and Sergey Zagoruyko. End-to-end object detection with transformers. In *European conference on computer vision*, pages 213–229. Springer, 2020.
- [4] Junsuk Choe, Seong Joon Oh, Seungho Lee, Sanghyuk Chun, Zeynep Akata, and Hyunjung Shim. Evaluating weakly supervised object localization methods right. In *Proceedings of the IEEE/CVF conference on computer vision and pattern recognition*, pages 3133–3142, 2020.

- [5] Junsuk Choe and Hyunjung Shim. Attention-based dropout layer for weakly supervised object localization. In *Proceedings of the IEEE/CVF Conference on Computer Vision and Pattern Recognition*, pages 2219–2228, 2019.
- [6] Zheng Huang, Kai Chen, Jianhua He, Xiang Bai, Dimosthenis Karatzas, Shijian Lu, and CV Jawahar. Icdar2019 competition on scanned receipt ocr and information extraction. In *2019 International Conference on Document Analysis and Recognition (ICDAR)*, pages 1516–1520. IEEE, 2019.
- [7] Wonseok Hwang, Seonghyeon Kim, Minjoon Seo, Jinyeong Yim, Seunghyun Park, Sungrae Park, Junyeop Lee, Bado Lee, and Hwalsuk Lee. Post-ocr parsing: building simple and robust parser via bio tagging. In *Workshop on Document Intelligence at NeurIPS 2019*, 2019.
- [8] Albert Q Jiang, Alexandre Sablayrolles, Arthur Mensch, Chris Bamford, Devendra Singh Chaplot, Diego de las Casas, Florian Bressand, Gianna Lengyel, Guillaume Lample, Lucile Saulnier, et al. Mistral 7b. *arXiv preprint arXiv:2310.06825*, 2023.
- [9] Albert Q Jiang, Alexandre Sablayrolles, Antoine Roux, Arthur Mensch, Blanche Savary, Chris Bamford, Devendra Singh Chaplot, Diego de las Casas, Emma Bou Hanna, Florian Bressand, et al. Mixtral of experts. *arXiv preprint arXiv:2401.04088*, 2024.
- [10] Glenn Jocher, Ayush Chaurasia, and Jiahui Qiu. Yolo by ultralytics. <https://github.com/ultralytics/ultralytics>, 2023.
- [11] Duy-Cuong Nguyen, Tuan-Anh Nguyen, and Xuan-Chung Nguyen. Mc-ocr challenge 2021: End-to-end system to extract key information from vietnamese receipts. In *2021 RIVF International Conference on Computing and Communication Technologies (RIVF)*, pages 1–5. IEEE, 2021.
- [12] Khang Tan Tran Minh Nguyen. Uit-mlreceipts: A multilingual benchmark for detecting and recognizing key information in receipts. *REV Journal on Electronics and Communications*, 14(1), 2024.
- [13] Thi Tuyet Hai Nguyen, Adam Jatowt, Mickael Coustaty, and Antoine Doucet. Survey of post-ocr processing approaches. *ACM Comput. Surv.*, 54(6), jul 2021.
- [14] Keiron O’shea and Ryan Nash. An introduction to convolutional neural networks. *arXiv preprint arXiv:1511.08458*, 2015.
- [15] Seunghyun Park, Seung Shin, Bado Lee, Junyeop Lee, Jaeheung Surh, Minjoon Seo, and Hwalsuk Lee. Cord: a consolidated receipt dataset for post-ocr parsing. In *Workshop on Document Intelligence at NeurIPS 2019*, 2019.
- [16] Chirag Patel, Atul Patel, and Dharmendra Patel. Optical character recognition by open source ocr tool tesseract: A case study. *International Journal of Computer Applications*, 55(10):50–56, 2012.
- [17] Krishna Kumar Singh and Yong Jae Lee. Hide-and-peek: Forcing a network to be meticulous for weakly-supervised object and action localization. In *International Conference on Computer Vision (ICCV)*, 2017.
- [18] Hugo Touvron, Louis Martin, Kevin Stone, Peter Albert, Amjad Almahairi, Yasmine Babaei, Nikolay Bashlykov, Soumya Batra, Prajjwal Bhargava, Shruti Bhosale, et al. Llama 2: Open foundation and fine-tuned chat models. *arXiv preprint arXiv:2307.09288*, 2023.
- [19] Lewis Tunstall, Edward Beeching, Nathan Lambert, Nazneen Rajani, Kashif Rasul, Younes Belkada, Shengyi Huang, Leandro von Werra, Clémentine Fourrier, Nathan Habib, et al. Zephyr: Direct distillation of lm alignment. *arXiv preprint arXiv:2310.16944*, 2023.
- [20] Xuan-Son Vu, Quang-Anh Bui, Nhu-Van Nguyen, Thi Tuyet Hai Nguyen, and Thanh Vu. Mc-ocr challenge: Mobile-captured image document recognition for vietnamese receipts. In *2021 RIVF International Conference on Computing and Communication Technologies (RIVF)*, pages 1–6. IEEE, 2021.

- [21] Chien-Yao Wang, Alexey Bochkovskiy, and Hong-Yuan Mark Liao. YOLOv7: Trainable bag-of-freebies sets new state-of-the-art for real-time object detectors. In *Proceedings of the IEEE/CVF Conference on Computer Vision and Pattern Recognition (CVPR)*, 2023.
- [22] Sangdoon Yun, Dongyoon Han, Seong Joon Oh, Sanghyuk Chun, Junsuk Choe, and Youngjoon Yoo. Cutmix: Regularization strategy to train strong classifiers with localizable features. In *International Conference on Computer Vision (ICCV)*, 2019.
- [23] Dingwen Zhang, Junwei Han, Gong Cheng, and Ming-Hsuan Yang. Weakly supervised object localization and detection: A survey. *IEEE transactions on pattern analysis and machine intelligence*, 44(9):5866–5885, 2021.
- [24] Hao Zhang, Feng Li, Shilong Liu, Lei Zhang, Hang Su, Jun Zhu, Lionel M Ni, and Heung-Yeung Shum. Dino: Detr with improved denoising anchor boxes for end-to-end object detection. *arXiv preprint arXiv:2203.03605*, 2022.
- [25] Xiaolin Zhang, Yunchao Wei, Jiashi Feng, Yi Yang, and Thomas Huang. Adversarial complementary learning for weakly supervised object localization. In *IEEE CVPR*, 2018.
- [26] Xiaolin Zhang, Yunchao Wei, Guoliang Kang, Yi Yang, and Thomas Huang. Self-produced guidance for weakly-supervised object localization. In *European Conference on Computer Vision*. Springer, 2018.
- [27] Bolei Zhou, Aditya Khosla, Agata Lapedriza, Aude Oliva, and Antonio Torralba. Learning deep features for discriminative localization. In *Proceedings of the IEEE conference on computer vision and pattern recognition*, pages 2921–2929, 2016.